Published in final edited form as:
Proc IEEE Int Symp Biomed Imaging. 2013 December 31; 2013: 226–229. doi:10.1109/ISBI.2013.6556453.

A POINT-CORRESPONDENCE APPROACH TO DESCRIBING THE DISTRIBUTION OF IMAGE FEATURES ON ANATOMICAL SURFACES, WITH APPLICATION TO ATRIAL FIBRILLATION

Gregory Gardner[★,†], **Alan Morris**[†], **Koji Higuchi**[†,‡], **Robert MacLeod**[★,†], and **Joshua Cates**[★,†]

[★]Scientific Computing and Imaging Institute University of Utah, Salt Lake City, UT, USA

[†]CARMA Center, University of Utah, Salt Lake City, UT, USA

[‡]University of Utah Hospital, Salt Lake City, UT, USA

Abstract

This paper describes a framework for summarizing and comparing the distributions of image features on anatomical shape surfaces in populations. The approach uses a point-based correspondence model to establish a mapping among surface positions and may be useful for anatomy that exhibits a relatively high degree of shape variability, such as cardiac anatomy. The approach is motivated by the MRI-based study of diseased, or *fibrotic*, tissue in the left atrium of atrial fibrillation (AF) patients, which has been difficult to measure quantitatively using more established image and surface registration techniques. The proposed method is to establish a set of point correspondences across a population of shape surfaces that provides a mapping from any surface to a common coordinate frame, where local features like fibrosis can be directly compared. To establish correspondence, we use a previously-described statistical optimization of particle-based shape representations. For our atrial fibrillation population, the proposed method provides evidence that more intense and widely distributed fibrosis patterns exist in patients that do not respond well to radiofrequency ablation therapy.

Index Terms

Correspondence; Atrial Fibrillation; LGE-MRI; Particle System

1. INTRODUCTION

In this work, we propose a framework for the summary and comparison of the distribution of local image features in a population of anatomical surfaces. The approach uses a point-based correspondence model of surface shape to establish a mapping among surfaces and may be especially useful for anatomy that exhibits relatively high variability in shape, such as cardiac anatomy. Our motivating application is an analysis of the distribution of *fibrosis*, or diseased tissue, in the left atrial (LA) walls of atrial fibrillation (AF) patient populations. Comparison of features on the LA wall is difficult due to the variability of anatomical structure [1] and unclear boundaries between adjacent anatomical structures. Moreover, the lack of consistent anatomical features across the LA surface makes even manual placement of landmarks unreliable. Conventional image-based registration techniques have also proven unreliable for this application because cardiac MRI suffers from inconsistent quality and appearance across subjects [2].

To compare image features on the LA wall, we propose to estimate a finite set of correspondence positions using the methods previously introduced by Cates, *et al.* in [3, 4,

5] for modeling anatomical shape. These methods automatically sample each surface in the population to produce a set of correspondences that is statistically optimal, in the sense that it minimizes the information content of the model while maintaining a good representation of shape surface geometry. The density of correspondence points can be adjusted to model geometric features at the scale appropriate for a given analysis. Once correspondence is established, an exact 1 – 1 mapping exists among all shapes, and image features may be compared at these points. Correspondence may also be estimated at any arbitrary surface position with a suitable interpolation, such as the radial basis function approach given by Bookstein [6].

Tissue changes in the LA wall are of particular interest for the study and treatment of AF, which is estimated to affect more than 10 million people worldwide by 2025 and is associated with a 5x increased risk of stroke [7, 8]. Numerous studies have shown that AF is accompanied by electrical and structural remodeling of the LA (see, *e.g.*, [9]) that leads to depletion of cardiac myocytes and an increase in pro-arrhythmic, collagenous tissue in the LA wall, termed *fibrosis*. Recently, late gadolinium enhanced magnetic resonance imaging (LGE-MRI) has been used to localize fibrosis in the LA. Clinicians use these LGE-MRI scans to guide catheter ablation procedures, where the sources of rogue electrical signals responsible for AF are cauterized with radiofrequency (RF) energy in a procedure known as RF ablation.

The extent of LA fibrosis is a major predictor of RF ablation success in AF patients [10]. Presumably, more diseased tissue in the LA requires more extensive ablation procedures to be successful. However, it is not well understood how the distribution of fibrosis within the LA affects RF ablation outcomes, nor are there standard methods for quantitative assessment of these distributions. Improved characterization of the LA tissue, by examining how fibrosis distributions vary across ablation outcomes, would allow clinicians to understand, and specifically target, fibrotic regions commonly observed in patients with failed procedures. To probe how fibrosis patterns vary with ablation outcomes, we divided the shape population based on ablation outcomes and generated the fibrosis distribution for successful and failed ablation procedures. Using the proposed methodology for feature comparison across LA surfaces, we found evidence that fibrotic tissue for AF patients is most prevalent on the posterior surface of the LA. Moreover, patients with failed RF-ablation treatments exhibit more intense and widespread distributions of fibrotic tissue. Insights such as these into the spatial distribution of fibrosis in AF may help to triage AF patients and better personalize their treatments by determining who will be better candidates for RF-ablation.

2. RELATED WORK

Current studies of LA fibrosis report the extent of fibrosis as a total percentage of LA wall volume, rather than describing its spatial distribution [10, 11]. Previous attempts to describe the distribution of LA fibrosis used optical mapping of isolated tissue or histological analysis of biopsies [12, 13]. However, the invasiveness of both approaches preclude their use in living subjects. Moreover, current analyses of fibrosis do not directly compare spatial distributions across subjects. Some work has been published on point-based correspondence for comparative studies of brain anatomy and local feature variability. One such study used point-based models to examine variations in local cortical features, such as sulcal depth, across subjects [5]. Cates *et al.* have proposed a system for establishing inter-subject correspondence without a parameterization of the surface or parameter tuning [3, 4]. This technique underlies the methodology of this paper and is discussed in more detail in Section 3.2.

3. METHODOLOGY

This section describes the proposed workflow for establishing inter-subject correspondence and its application to the analysis of fibrotic tissue distribution in patients with AF. First, LGE-MRI scans are acquired for each patient. Then the anatomical regions of interest are delineated by manual expert segmentation, which are then smoothed and roughly aligned using gross anatomical features. The point-based correspondences are established directly from the aligned volumes using an entropy-based optimization method. Finally, the presence of fibrotic tissue in a spherical neighborhood around each correspondence point is measured and then mapped to the mean shape – or any other representative LA shape – in the correspondence model (Figure 1). The workflow presented in this paper is generic and modular; the different stages of this pipeline can be substituted with other methods based on application-specific needs.

3.1. Patient Selection and Image Acquisition

For this study, we selected 160 AF patients retrospectively (mean age: 66 ± 11 years, 103 males) who presented to the University of Utah for catheter ablation. Patient information gathered for the purposes of the study was de-identified and protected in compliance with HIPAA regulations. All patients underwent a LGE-MRI evaluation prior to ablation to assess the extent of atrial fibrosis. Only patients without prior ablations were included because the scarring induced by ablation procedures confounds detection of atrial fibrosis. Image acquisition was performed using a MAGNETOM Verio 3-T clinical MRI scanner (Siemens Medical Solutions, Erlangen, Germany). The MRI contrast agent gadolinium (0.1 mmol/kg; Multihance, Bracco Diagnostic Inc., Princeton, NJ) was injected approximately 15 minutes prior acquisition of the LGE-MRI images. The poor washout kinetics of gadolinium in injured tissue causes regions of diseased tissue *e.g.*, fibrosis, to appear as bright voxels in the LGE-MRI scans. The typical acquisition parameters for the LGE-MRI scans are described in detail in [11]. Recurrence of AF, signifying a failed ablation, was defined as any episode of AF longer than 30 seconds that occurred at least 3 months post-ablation. Recurrence of AF was observed in 57 patients.

3.2. Establishing Point-Based Corresondence

To produce the correspondence model of LA shape, which defines the mapping between surface points, we computed 512 correspondence points on each LA surface using the particle-based method proposed by Cates, *et al.* [3]. This method models surfaces as particle systems and optimizes their configurations by balancing the information content in each shape representation against the information content of the population of shapes. The inputs to the correspondence computation are aligned distance transforms from binary segmentation volumes, which form implicit object surface representations.

In our study, the boundaries of the LA myocardium were manually segmented by experts using the Corview cardiac segmentation and analysis software (CARMA Center, University of Utah, www.corview.org). We thresholded the enhancement in the original LGE-MRI image to localize the fibrosis within the LA wall [14]. We aligned the segmentations, with respect to translation, by shifting their origins to their center of mass. We assume a rough rotational alignment because all patients are positioned in the same orientation in the scanner. Later, during the optimization, this initial alignment is refined using the Procrustes algorithm to remove residual, non-shape pose parameters (as described in [4]).

The LA segmentations contain an implicit shape surface at the boundary between the labeled pixels in the region of interest and the background pixels. To alleviate aliasing artifacts at this boundary, we applied an antialiasing algorithm that also preserves the position of

surface boundaries [15]. Antialiasing was followed by a very slight Gaussian blur operation to remove high-frequency artifacts arising from numerical approximations. We note that the location of the segmentation boundaries is not appreciably altered by filtering and remained accurate to within two pixels.

3.3. Evaluating Correspondence Accuracy

As a measure of the correspondence model's accuracy, we mapped manually-determined landmarks to the population's mean shape and analyzed their distributions. The mean shape is computed as the set of average positions of each correspondence point across the population of shapes. The landmarks consist of the following: the center of the mitral valve and the insertion sites of the LA appendage and 4 pulmonary veins for 18 randomly selected patients from the population. The continuous coordinate transformations to map landmarks to the mean shape were derived using a 3D extension of the thin-plate spline correspondence point interpolation proposed by Bookstein [6].

3.4. Computing Fibrosis Distributions

Experts segmented the fibrotic tissue in the LA wall of each subject using the raw LGE-MRI data and a threshold-based approach described previously in [14]. Using the fibrosis classifications in the LA wall, we can estimate the distribution of fibrosis on the LA surface as a histogram of the presence of fibrosis at each correspondence point position. The surface histogram is computed as follows: for each correspondence position, we record the number of times that fibrosis is seen in the region of that correspondence point (2.5mm radius) over the whole population of shapes. The histogram can then be visualized on a representative shape (such as the mean or median shape) to show the patterning of fibrosis in the population. Additionally, we can compute histograms for sub-populations and compare their distributions. In this study we compare the fibrosis histograms for two populations: AF patients who have successful RF ablation outcomes and AF patients with unsuccessful RF ablation outcomes, where success is defined by freedom from AF events at 3 months.

4. RESULTS

Figure 2 illustrates some representative LA shapes with correspondence points displayed as small spheres on the surface. The gray structures are the LA appendage and the pulmonary vein insertion sites, which are also the common anatomical landmarks chosen for the accuracy assessment described in Section 3.3. Panel a. in Fig. 2 shows the observed spatial distribution of fibrosis on the posterior LA surface in patients with a successful ablation procedure; panel b. shows the distribution in patients who relapsed into AF. Panel c. shows the difference between the two groups, measured as the percentage of recurrent patients minus nonrecurrent patients exhibiting fibrosis at each point. The posterior LA surface showed less intense and widespread fibrosis with successful ablations.

Table 1 describes the distribution of the manually-chosen landmarks after mapping to the mean shape of the correspondence model. The native resolution of the original LGE-MRI scans is 1.25mm × 1.25mm × 2.5mm. From this analysis, we conclude that the average variability in the landmarks is on the order of two pixels and our correspondence method is accurate enough for the purpose of describing fibrosis distributions in these data. Note that our accuracy metric does not separate the inherent variability in manual landmark selection. The higher variability of the mitral valve landmarks, for example, is possibly due to its larger area and the difficulty of consistently locating its center. Subjective inspection of the fibrosis distributions also shows little to no fibrosis present in the mitral valve region of the common shape, which is encouraging as this region does not consist of myocardium, and hence fibrosis.

5. DISCUSSION

In this paper we have proposed a correspondence-based approach to the comparison of image-derived features on shape surfaces that can be successfully applied to the relatively complex anatomy of the left-atrium. The correspondence model allows locally interesting features to be tabulated on a representative shape, such as the mean shape, revealing spatial distributions of local features across the population. The accuracy of the correspondence model may also be assessed in an application-specific way by examining the variability of manually-determined landmarks within this common coordinate frame. Our analysis of fibrosis distributions in the LA of AF patients has shown fibrotic tissue to be most prevalent on the posterior surface of the LA. Additionally, patients with poor RF ablation outcomes exhibit a more intense and widespread distribution of fibrosis across the posterior LA surface.

Future work remains to better assess the accuracy of this approach. Several more extensive studies are warranted: an analysis of the tradeoff between surface sampling density and accuracy; assessment of accuracy relative to manual landmark variability; and a comparison of this correspondence-based approach with deformable surface registration techniques, in particular for highly variable anatomy, such as the LA.

References

1. Karim, R.; Rueckert, D.; Mohiaddin, R.; Drivas, P. Biomedical Imaging: From Nano to Macro, ISBI 2009. IEEE; 2009. Automatic extraction of the left atrial anatomy from MR for atrial fibrillation ablation; p. 502-505.
2. Makela T, Clarysse P, Sipila O, et al. A review of cardiac image registration methods. IEEE Trans Med Imaging. 2002; 21(9):1011–1021. [PubMed: 12564869]
3. Cates J, Meyer M, Fletcher PT, Whitaker R. Entropy-based particle systems for shape correspondence. Proc MICCAI Mathematical Foundations of Computational Anatomy Workshop. 2006:90–99.
4. Cates, J.; Fletcher, P.; Styner, M., et al. Information Processing in Medical Imaging. Springer; 2007. Shape modeling and analysis with entropy-based particle systems; p. 333-345.
5. Oguz, I.; Cates, J.; Fletcher, T., et al. Biomedical Imaging: From Nano to Macro ISBI 2008. IEEE; 2008. Cortical correspondence using entropy-based particle systems and local features; p. 1637-1640.
6. Bookstein FL. Principal warps: Thin-plate splines and the decomposition of deformations. IEEE Trans Pattern Anal Mach Intell. 1989; 11(6):567–585.
7. Miyasaka Y, Barnes ME, Gersh BJ, et al. Secular trends in incidence of atrial fibrillation in olmsted county, minnesota, 1980 to 2000, and implications on the projections for future prevalence. Circulation. 2006; 114(2):119–125. [PubMed: 16818816]
8. Benjamin EJ, Levy D, Vaziri SM, et al. Independent risk factors for atrial fibrillation in a population-based cohort. J Am Med Assoc. 1994; 271(11):840–844.
9. Allessie M, Ausma J, Schotten U. Electrical, contractile and structural remodeling during atrial fibrillation. Cardiovasc Res. 2002; 54(2):230–246. [PubMed: 12062329]
10. Akoum N, Daccarett M, McGann CJ, et al. Atrial fibrosis helps select the appropriate patient and strategy in catheter ablation of atrial fibrillation: A DE-MRI guided approach. J of Cardiovasc Electr. 2011; 22(1):16–22.
11. McGann CJ, Kholmovski EG, Oakes RS, et al. New magnetic resonance imaging-based method for defining the extent of left atrial wall injury after the ablation of atrial fibrillation. J Am Coll Cardiol. 2008; 52(15):1263–1271. [PubMed: 18926331]
12. Tanaka K, Zlochiver S, Vikstrom KL, et al. Spatial distribution of fibrosis governs fibrillation wave dynamics in the posterior left atrium during heart failure. Circ Res. 2007; 101(8):839–847. [PubMed: 17704207]

13. Boldt A, Wetzel U, Lauschke J, et al. Fibrosis in left atrial tissue of patients with atrial fibrillation with and without underlying mitral valve disease. Heart. 2004; 90(4):400–405. [PubMed: 15020515]

14. Oakes RS, Badger TJ, Kholmovski EG, et al. Detection and quantification of left atrial structural remodeling with delayed-enhancement magnetic resonance imaging in patients with atrial fibrillation. Circulation. 2009; 119(13):1758–1767. [PubMed: 19307477]

15. Williams J, Rossignac J. Tightening: Morphological simplification. Int J Comput Geom Ap. 2007; 17(05):487–503.

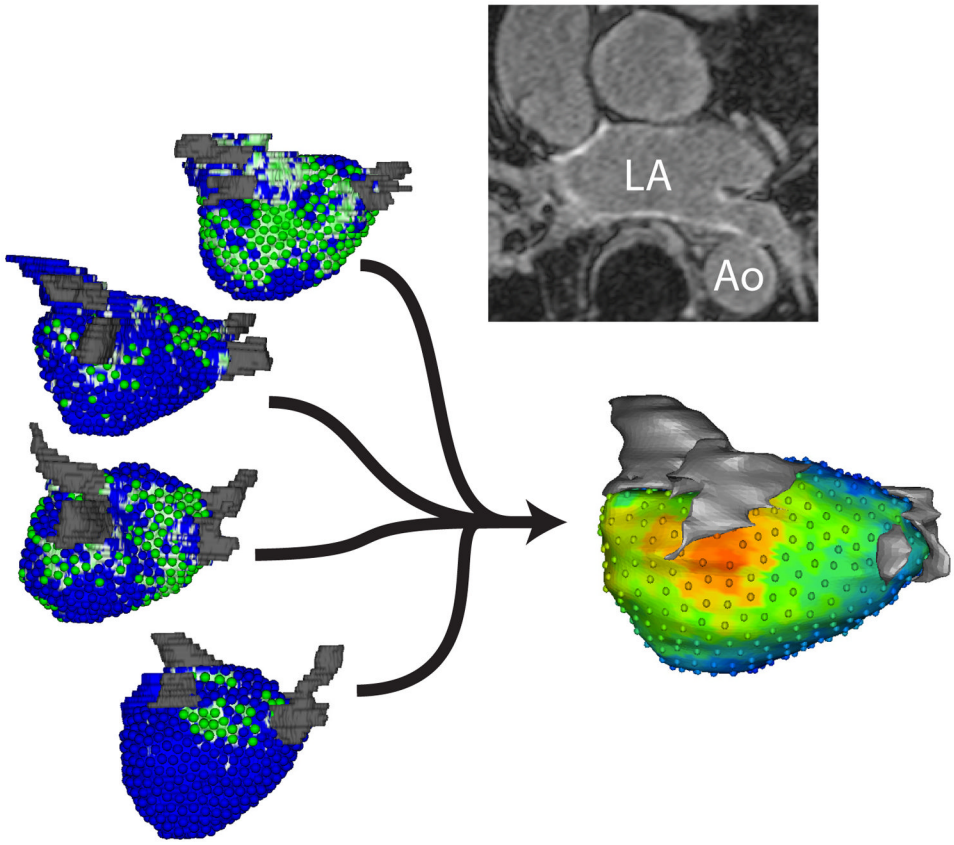

Fig. 1.
Workflow overview. A LGE-MRI is shown top right (Ao denotes aorta). Below, fibrosis (green patches) from patient volumes is mapped into the common coordinate system.

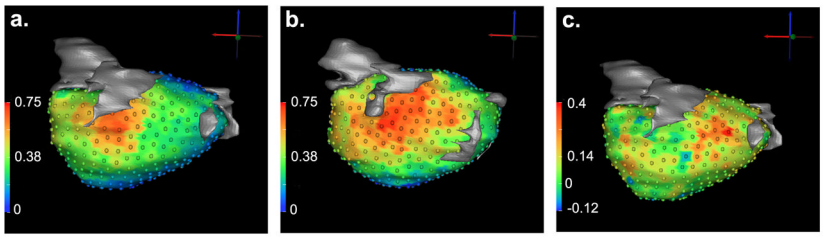

Fig. 2.

Ablation success and spatial distribution of fibrosis. The LA posterior surface is shown in patients with (a.) successful and (b.) poor outcomes. (c.) Patients with failed ablations showed higher percentages of fibrosis at most correspondence points.

Table 1

Landmark Distributions

Landmark	Mean ± Std. Dev. (mm)
Pulmonary Veins	5.59 ± 1.94
LA Appendage	6.36 ± 2.15
Mitral Valve	6.90 ± 3.56